Regions of Stability for Limit Cycles of Piecewise Linear Systems

Jorge M. Gonçalves
California Institute of Technology
CDS, MC 107-81, Pasadena, CA 91125
jmg@cds.caltech.edu
http://www.cds.caltech.edu/∼jmg/

***Abstract*— This paper starts by presenting local stability conditions for limit cycles of piecewise linear systems (PLS), based on analyzing the linear part of Poincaré maps. Local stability guarantees the existence of an asymptotically stable neighborhood around the limit cycle. However, tools to characterize such neighborhood do not exist. This work gives conditions in the form of LMIs that guarantee asymptotic stability of PLS in a reasonably large region around a limit cycle, based on recent results on impact maps and surface Lyapunov functions (SuLF). These are exemplified with a 4^{th}–order neural oscillator, also used in many robotics applications like, for example, juggling and locomotion.**

I. INTRODUCTION

Piecewise linear systems (PLS) are characterized by a finite number of linear dynamical models together with a set of rules for switching among these models. This captures discontinuity actions in the dynamics from either the controller or system nonlinearities. Although widely used and intuitively simple, PLS are computationally hard and only recently there has been some interesting results. In the analysis of equilibrium points of PLS, [4], [7], [11] construct piecewise quadratic Lyapunov functions in the state space, and [2], alternatively, constructs Lyapunov functions on the switching surfaces (SuLF) associated with the system.

Many PLS, however, have limit cycles. For a large class of relay feedback systems [1], one of the simplest PLS, there will be limit cycle oscillations. Such systems can be found in numerous applications like electromechanical systems, simple models of dry friction, delta-sigma modulators, automatic tuning of PID regulators. Walking can also be seen as an oscillatory motion [12]. Walking robots are typically designed to walk at some predetermined velocity which is to be maintained even in the presence of external perturbations. In biology, oscillations appear in several applications like cell cycle [8], excitable cells like cardiac cells [8], circadian rhythms [3], and neural oscillators [9]. Neural oscillators are also used in many robotics applications like, for example, juggling [14] and bipedal locomotion control [5]. Here, the oscillator, composed of a PLS, is connected in feedback with the robot to induce oscillations.

Local stability of limit cycles of PLS can easily be checked by linearizing the Poincaré map. However, global stability or even characterization of stability in regions around limit cycles cannot, in general, be checked or found. Simulations and experiments are typically the only way to have an idea about the stability of the system. [13] constructs local quadratic Lyapunov functions and then checks what regions of stability they guarantee. This check, however, is in general computationally hard and becomes impracticable for systems of order higher than 2. The results in [7] do not apply since Lyapunov functions cannot be constructed in the state space to prove stability of limit cycles. We then turn to construct Lyapunov functions on switching surfaces (SuLF). In the past, such construction seemed like an impossible task since impact maps, i.e., maps from one switch to the next, are, in general, nonlinear, multivalued, and not continuous. The work by [2], however, introduced a new and simple way to construct SuLF by simply solving a set of LMIs, and proving this way global stability of several classes of PLS.

There are, however, many applications that do not require checking global stability, either because this is very expensive or maybe the system is not defined everywhere. Models of walking robots, for instance, are typically only defined in some region of the state space. This paper investigates the problem of constructing reasonably large regions of stability around a limit cycle. Trajectories starting in this region are guaranteed to converge asymptotically to the limit cycle. This is done in two steps. First, impact maps are found to be contractive in the large as possible set of switching times. Then, invariant ellipsoids on switching surfaces are characterized. The method is exemplified with a $4th$–order neural oscillator [9].

The remainder of this paper is organized as follows. Section II describes the problem to be solved, and gives existence and local stability results for limit cycles of PLS. Section III presents the main result of this paper followed by an example in section IV. Proofs of all results can be found in section V. Finally, conclusions can be found in section VI.

II. PROBLEM DESCRIPTION

Piecewise linear systems (PLS) are characterized by a set of affine linear systems

$$\dot{x} = A_i x + B_i \tag{1}$$

where $x \in \mathbb{R}^n$ is the state, together with a switching rule

$$i(x) \in \{1, ..., M\} \tag{2}$$

that depends on present and possibly also on past values of x. By a solution of (1)-(2) we mean functions (x, i) satisfying (1)-(2), where $i(t)$ is piecewise constant. t is a *switching time* of a solution of (1)-(2) if $i(t)$ is discontinuous

at t. We say a trajectory of (1)-(2) *switches* at some time t if t is a switching time. In the state space, switches occur at *switching surfaces* consisting of hyperplanes of dimension $n-1$

$$S_i = \{x|\ C_i x + d_i = 0\}$$

where C_i is a row vector and $i = \{1,...,N\}$.

This paper assumes that existence of solution is always guaranteed for any initial condition. See [6] for conditions on existence of solutions for PLS.

A. Limit Cycles

Unlike linear systems that only have a single equilibrium point, PLS may exhibit multiple equilibrium points and/or limit cycles. Here, we are interested in limit cycles. For the remainder of the paper, assume the PLS (1)-(2) has a limit cycle γ with period t^*, and that this limit cycle crosses transversely[1] k switching surfaces per cycle. For simplicity, and without loss of generality, assume the trajectory of the limit cycle evolves consecutively from system 1, to system 2, and so forth until it reaches system k and, finally, after completing one cycle, returns to system 1. Assume also the switching surfaces are ordered the same way (see figure 1). This means the trajectory $\phi(t)$ of the limit cycle, starting at $x_1^* \in S_1$, satisfies $\phi(t_1^*) = x_2^* \in S_2$. Then system 2 "takes over" until $\phi(t_1^* + t_2^*) = x_3^* \in S_3$, and so on. The last affine linear system k takes the trajectory $\phi(t)$ from $x_k^* \in S_k$ back to $x_1^* \in S_1$, i.e., $\phi(t_1^* + t_2^* + \cdots + t_k^*) = x_{k+1}^* = x_1^* \in S_1$. Note that $t^* = t_1^* + t_2^* + \cdots + t_k^*$. Note also that there is no loss of generality in this characterization of a limit cycle. If, for instance, the limit cycle crosses the same switching surface more than once, we simply have $S_i = S_j$ for some i, j. For convenience, indexes $k+1$ and 1 represent the same object, i.e., $x_{k+1}^* = x_1^*$, $S_{k+1} = S_1$, etc.

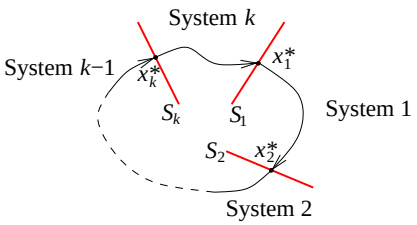

Fig. 1. Limit cycle γ

1) Existence of Limit Cycles: Next are conditions for the existence of limit cycles of PLS. For simplicity, we will first study the case where the limit cycle has only two switches per cycle, i.e., $k = 2$. Then, the result is extended to k switches. Also, for simplicity, assume the A_i matrices are invertible, although this is not necessary.

[1] ϕ is *transversal* to $S = \{x|\ Cx = d\}$ at $p = \phi(t) \in S$ if $C\dot{\phi}(t-0) \neq 0$. This is necessary or otherwise the limit cycle would be unstable.

Proposition 2.1: Consider the PLS (1)-(2). Assume there exists a periodic solution γ with two switches per cycle and period $t^* = t_1^* + t_2^* > 0$. Define

$$\begin{aligned} x_1^* &= \left(I - e^{A_2 t_2^*} e^{A_1 t_1^*}\right)^{-1} \left[e^{A_2 t_2^*}(e^{A_1 t_1^*} - I)A_1^{-1}B_1 \right. \\ &\qquad \left. + (e^{A_2 t_2^*} - I)A_2^{-1}B_2\right] \\ x_2^* &= \left(I - e^{A_1 t_1^*} e^{A_2 t_2^*}\right)^{-1} \left[e^{A_1 t_1^*}(e^{A_2 t_2^*} - I)A_2^{-1}B_2 \right. \\ &\qquad \left. + (e^{A_1 t_1^*} - I)A_1^{-1}B_1\right] \end{aligned}$$

and $g_1(t_1^*, t_2^*) = C_1 x_1^* + d_1$, $g_2(t_1^*, t_2^*) = C_2 x_2^* + d_2$. Then the following conditions hold

$$\begin{cases} g_1(t_1^*, t_2^*) = 0 \\ g_2(t_1^*, t_2^*) = 0 \end{cases} \tag{3}$$

and the periodic solution is governed by system 1 on $[0, t_1^*)$, and by system 2 on $[t_1^*, t^*)$. Furthermore, the periodic solution γ is obtained with either initial conditions x_1^*, x_2^*.

Example 2.1: For visualization purposes, consider two affine linear systems in $\mathbb{R}^2$, $\dot{x} = A_i x + B_i$ where

$$A_1 = A_2 = \begin{pmatrix} -1 & 0 \\ 0 & -2 \end{pmatrix}, \quad B_1 = \begin{pmatrix} -3 \\ -2 \end{pmatrix}, \quad \text{and} \quad B_2 = \begin{pmatrix} 2 \\ 2 \end{pmatrix}$$

together with a switching rule with memory that uses system 1 until the trajectory intersects the switching surface S_1, and then uses system 2 until the trajectory intersects the switching surface S_2, and so on. The switching surfaces are given by $C_1 = (-1 \ \ 1)$, $d_1 = -1$, $C_2 = (1 \ \ 0)$, and $d_2 = -1$. Solving (3) numerically yields $t_1^* = 1.24$, $t_2^* = 1.35$, $x_1^* = x_3^* = (1 \ \ 0.87)'$, $x_2^* = (-1.84 \ \ -0.84)'$. The resulting periodic solution γ can be seen in figure 2. ■

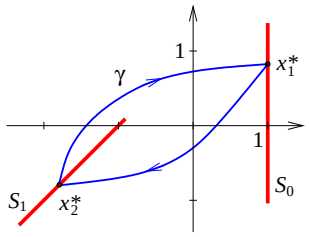

Fig. 2. Periodic solution of a second-order PLS

This result can be generalized to the case where a periodic solution γ switches among k systems instead of just two. For simplicity of notation let $E_i = e^{A_i t_i^*}$ and $z_i = A_i^{-1} B_i$. Define

$$x_1^* = \left(I - E_k \cdots E_1\right)^{-1} \left[\sum_{i=1}^{k-1} E_k \cdots E_{i+1}(E_i - I)z_i + (E_k - I)z_k\right]$$

where x_1^* was found based on the switching sequence $\{1, 2, ..., k\}$. To find, x_j^*, $j = 2, ..., k$, consider the switching sequence $\{j, ..., k, 1, ..., j-1\}$, i.e., just replace the indexes in x_1^* the following way: 1 by j, 2 by $j+1$ (or by 1 if $j+1 > k$), up to k by $j-1$. Finally, define $g_j = C_j x_j^* + d_j$.

Proposition 2.2: Consider the PLS (1)-(2). Assume there exists a periodic solution γ with k switches per cycle and period $t^* = t_1^* + t_2^* + \cdots t_k^* > 0$. Consider the functions $g_1, g_2, ..., g_k$ defined as above. Then the following conditions hold

$$\begin{cases} g_1(t_1^*, t_2^*, ..., t_k^*) &= 0 \\ g_2(t_1^*, t_2^*, ..., t_k^*) &= 0 \\ \vdots & \\ g_k(t_1^*, t_2^*, ..., t_k^*) &= 0 \end{cases} \tag{4}$$

and the periodic solution is governed by system 1 on $[0, t_1^*)$, and by system i on $[t_1^* + \cdots + t_{i-1}^*, t_1^* + \cdots + t_i^*)$, $i = 2, ..., k$. Furthermore, the periodic solution γ can be obtained with the initial condition $x_1^* \in S_1$.

As in the case where $k = 2$, (4) is a set of transcendental equations. Closed form solutions can only be given for very special cases and, even numerically, this is a hard problem. An alternative is to simulate the system for some time to get approximate values for $t_1^*, t_2^*, ..., t_k^*$, and then use some numerical algorithm to precisely compute $t_1^*, t_2^*, ..., t_k^*$.

2) Local Stability: Consider the Poincaré map T from some point in a small neighborhood of x_1^* in S_1, to the point where the trajectory returns to S_1. The limit cycle is locally stable if the eigenvalues of the Jacobian of T are inside the unit disk.

Proposition 2.3: Consider the PLS (1)-(2). Assume there exists a limit cycle γ with period t^*. The Jacobian of the Poincaré map T is given by $W = W_k W_{k-1} \cdots W_2 W_1$ where

$$W_i = \left(I - \frac{v_i C_{i+1}}{C_{i+1} v_i} \right) e^{A_i t_i^*}$$

with $v_i = A_i x_{i+1}^* + B_i$, $i = 1, ..., k$. The limit cycle γ is locally stable if W has all its eigenvalues inside the unit disk. It is unstable if at least one of the eigenvalues of W is outside the unit disk.

Example 2.2: Returning to example 2.1, W can be computed from W_1 and W_2, yielding

$$W = 10^{-3} \begin{pmatrix} 0 & 0 \\ -0.29 & 0.32 \end{pmatrix}$$

which has all its eigenvalues inside the unit disk. Therefore the limit cycle in example 2.1 is locally stable. ■

If, with the above proposition, a limit cycle γ is proven locally stable, then there exist a neighborhood in S_1 around x_1^* such that any trajectory starting in this neighborhood will converge asymptotically to the limit cycle γ. However, the proposition does not characterize in any way this neighborhood since it only considers the Jacobian of the Poincaré map and neglects all other high-order terms. Those high-order terms carry the necessary information to characterize the stable neighborhood. Next, we show how to characterize a reasonably large stable region around a locally stable limit cycle (see figure 3).

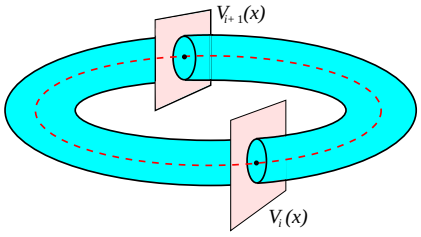

Fig. 3. Region of stability around a limit cycle

III. MAIN RESULTS

This section is divided in two parts. First, it focuses on the analysis of a single impact map. Then, it uses this information to analyze the limit cycle.

A. Analysis of a single impact map

Lets start by parameterizing vectors $x_i \in S_i$ at switching surfaces. Write $x_i = x_i^* + \Pi_i \Delta_i$, where $\Pi_i = C_i^\perp$ ($C^\perp$ stands for the orthogonal complement of C) and $\Delta_i \in \mathbb{R}^{n-1}$.

Consider impact map i, i.e., the map from some $U_i \subset S_i$ to the next switch at S_{i+1}. The set U_i, to be found later, must be such that impact map i is a contraction and continuous in U_i, and $x_i^* \in U_i$. Let $\mathscr{T}_i$ be the set of all switching times of points in U_i. Since $x_i^* \in U_i$, $t_i^* \in \mathscr{T}_i$. The set U_i will be found in two steps. *Step 1* finds the largest set of switching times $\mathscr{T}_i$ for which the impact map is a contraction. *Step 2* characterizes the set U_i as the largest ellipsoid around x_i^* where the impact map is continuous and each point in U_i has a switching time in $\mathscr{T}_i$. We start with *Step 1*.

Although typical impact maps are nonlinear and hard to characterize, we found [2] that they can be expressed as a linear transformation parametrized by the switching time. Define $x_i^*(t)$ as the trajectory of (1), starting at x_i^*, for all $t \geq 0$ and

$$H_i(t) = \Pi_{i+1}' \left[I + \frac{(x_i^*(t) - x_{i+1}^*) C_{i+1}}{d_{i+1} - C_{i+1} x_i^*(t)} \right] e^{A_i t} \Pi_i$$

for all $t \in \mathscr{T}_i$ (note that at $t = t_i^*$, $H(t)$ is defined by the limit as $t \to t_i^*$). Then, for any $\Pi_i \Delta_i \in U_i - x_i^*$ there exists a $t \in \mathscr{T}_i$ such that the impact map is given by

$$\Delta_{i+1} = H_i(t) \Delta_i \tag{5}$$

Such t is the switching time associated with Δ_{i+1}.

To check contraction of impact maps, let V_i be polynomial Lyapunov functions defined on $\mathbb{R}^{n-1}$, with $V_i(0) = 0$ and $V_i(\Delta) > 0$, $\Delta \neq 0$. Contraction of impact map i follows if

$$V_i(\Delta_i) - V_{i+1}(H_i(t)\Delta_i) > 0 \tag{6}$$

for all $\Pi_i \Delta_i \in U_i - x_i^*$ and corresponding switching time $t = t(\Delta_i)$. The above inequality can be relaxed to an LMI parametrized by t. For instance, if V_i is chosen quadratic, i.e., $V_i(x) = x' P_i x$, $P_i > 0$, then contraction follows if

$$P_i - H_i'(t) P_{i+1} H_i(t) > 0 \tag{7}$$

for all $t \in \mathscr{T}_i$. If V_i is chosen as another higher-order polynomial Lyapunov function, then (6) can be relaxed to an LMI by expressing (6) as a sum of squares (see [10] for details). Therefore, *Step 1* finds the largest set of switching times $\mathscr{T}_i$ such that (7) is satisfied.

The first part of *Step 2* consists of finding the largest ellipsoid in S_i around x_i^* where impact i is continuous. Note that, by assumption, the limit cycle is transversal at switching surfaces. Thus, by the implicit function theorem, each impact map i is guaranteed to be continuous in some neighborhood of x_i^*. Define $C_t = C_{i+1}e^{A_i t}\Pi_i$ and $d_t = d_{i+1} - C_{i+1}x_i^*(t)$. For any $P > 0$, let $\|x\|_P^2 = x'Px$.

Lemma 3.1: Given $P_i = P_i' > 0$ and a set of switching times $\mathscr{T}_i = [t_{i-}, t_{i+}]$, define

$$R_i^c = \min_{t \in \mathscr{T}_i} \frac{|\dot{d}_t|}{\sqrt{\dot{C}_t P_i^{-1} \dot{C}_t}}$$

Then, the impact from $\{x_i^* + \Pi_i\Delta_i : \|\Delta_i\|_{P_i} < R_i^c \text{ and } t \in \mathscr{T}_i\}$ to S_{i+1} is continuous.

Remember that the proofs of all results can be found in section V. The second part of *Step 2* consists of finding a set of initial conditions characterized by an ellipsoid in S_i such that every point in that set has switching times in $\mathscr{T}_i$. There are many ways to find such ellipsoids. Next, we present two.

Lemma 3.2: Let $P_i = P_i' > 0$ and $r > 0$, and define

$$\bar{R}_i = \min_{t - t_i^* \in [-r,r]} \frac{\left|\frac{d_t}{t - t_i^*}\right| r}{\|C_t'\|_{P_i^{-1}}}$$

Let $R_i = \min\{\bar{R}_i, R_i^c\}$. Then, $\|\Delta_i\|_{P_i} < R_i$ implies $|t - t_i^*| \le r$.

In many situations (especially when A is Hurwitz), the following lemma gives a less conservative R_i.

Lemma 3.3: Given $P_i = P_i' > 0$ and a set of switching times $\mathscr{T}_i = [t_{i-}, t_{i+}]$, define

$$\bar{R}_i = \inf_{t \notin \mathscr{T}_i} \frac{|d_t|}{\|C_t'\|_{P_i^{-1}}}$$

Let $R_i = \min\{\bar{R}_i, R_i^c\}$. Then, $\|\Delta_i\|_{P_i} < R_i$ implies $t \in \mathscr{T}_i$.

Hence, we pick the largest R_i from lemmas 3.2 and 3.3. Next, we summarize both *Step 1* and *Step 2*.

Theorem 3.1: Consider impact map i. Assume (6) is satisfied for all $t \in [t_{i-}, t_{i+}]$. Let R_i be the largest from both lemmas 3.2 and 3.3. Then, the impact map in the domain $\{x_i^* + \Pi_i\Delta_i : \|\Delta_i\|_{P_i} < R_i\}$ is a contraction.

B. Regions of stability for limit cycles

Assume the PLS (1)-(2) has a locally stable limit cycle γ with period t^*, and that this limit cycle crosses transversely k switching surfaces per cycle. To analyze the limit cycle, all k impact maps associated with the limit cycle need to be simultaneously analyzed.

Theorem 3.2: Let $\mathscr{T}_i$ be the largest sets such that

$$V_i(\Delta_i) - V_{i+1}(H_i(t_i)\Delta_i) > 0, \quad t_i \in \mathscr{T}_i, \quad i = 1, \ldots, k \qquad (8)$$

Find R_i to be the largest between lemmas 3.2 and 3.3, $i = 1, \ldots, k$. Let $R = \min\{R_i\}$. Then trajectories starting inside of any of the ellipses defined by $\{x_i^* + \Pi_i\Delta_i : \|\Delta_i\|_{P_i} < R_i\} \subset S_i$, $i = 1, \ldots, k$, converge asymptotically to the limit cycle γ.

Condition (8) can be reduced to k infinite dimensional LMIs. Note that each of these LMIs is parametrized by a single switching time t_i. Thus, each can be gridded individually to obtain a set of finite dimensional LMIs [2].

IV. EXAMPLE

This is an example of a biological application known as a neural oscillator. It consists of two neurons in mutual inhibition producing a limit cycle oscillation [9]. In robotics, this oscillator is also used in feedback with systems requiring an oscillatory behavior [5], [14] . The neural oscillator is a $4th$–order system with states $x = (x_1\ x_2\ x_3\ x_4)'$ given by

$$\begin{cases} \dot{x}_1 &= -10x_1 - 20x_2 - 20[x_3]^+ + 10 \\ \dot{x}_2 &= 5[x_1]^+ - 5x_2 \\ \dot{x}_3 &= -20[x_1]^+ - 10x_3 - 20x_4 + 10 \\ \dot{x}_4 &= 5[x_3]^+ - 5x_4 \end{cases}$$

where $[u]^+ = \max\{0, u\}$ is an on/off controller, and x_1, x_3 are the firing rates of each neuron. Due to the on/off nonlinearities, the state space is divided in four regions where the system is (affine) linear. The system has a locally stable limit cycle that switches four times per cycle with period $t^* \approx 0.16 + 0.29 + 0.16 + 0.29$. The intersection of the limit cycle with the switching surfaces occurs at $x_1^* \approx (0.34\ \ 0.35\ \ 0\ \ 0.06)'$, $x_2^* \approx (0\ \ 0.26\ \ 0.4\ \ 0.14)'$, $x_3^* \approx (0\ \ 0.06\ \ 0.34\ \ 0.35)'$ and $x_4^* \approx (0.4\ \ 0.14\ \ 0\ \ 0.26)'$. Since the switches do not depend on the state variables x_2 and x_4, for visualization purposes the limit cycle can be projected onto the x_1, x_3 subspace (see the left side of figure 4). Note that in $\mathbb{R}^4$ the limit cycle does not actually crosses itself.

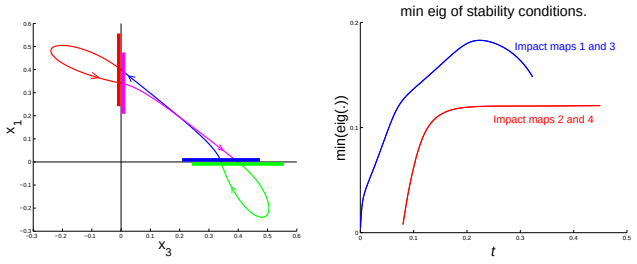

Fig. 4. Limit cycle of the neural oscillator projected onto the x_1, x_3 subspace (left); Minimum eigenvalues of conditions (7) for each impact map (right).

Step 1 consists of finding the largest switching time sets for which conditions (8) are satisfied. Using quadratic SuLF, conditions (7) were satisfied on $\mathscr{T}_1, \mathscr{T}_3 = [0, 0.32]$ and $\mathscr{T}_2, \mathscr{T}_4 = [0.08, 0.45]$, which can be seen on the right side of figure 4. Note that impact maps 1 and 3 and impact maps 2 and 4 coincide since there is a symmetry in the system around the axes $x_1 = x_3$ and $x_2 = x_4$. *Step 2* consists of finding the maximum possible R using lemmas 3.2 and 3.3. The regions

of stability can be seen on the left of figure 4 (projected onto the x_1, x_3 subspace), defining reasonably large regions around the limit cycle.

V. PROOF OF RESULTS

This section is dedicated to prove all the propositions and lemmas in the paper, starting with propositions 2.1, 2.2, and 2.3, and then lemmas 3.1, 3.2, and 3.3.

Proof of proposition 2.1: Let's first find g_1. Integrating (1) for the first system yields

$$x(t) = e^{A_1 t}(x(0) + A_1^{-1}B_1) - A_1^{-1}B_1$$

If $x(0) = x_1^* \in S_1$ is a point in γ then

$$x_2^* = e^{A_1 t_1^*}(x_1^* + A_1^{-1}B_1) - A_1^{-1}B_1$$

where $x_2^* \in S_2$. In a similar way, for the second system

$$x_3^* = e^{A_2 t_2^*}(x_2^* + A_2^{-1}B_2) - A_2^{-1}B_2$$

Replacing x_2^* in the previous equation and noticing that $x_3^* = x_1^*$ yields

$$x_1^* = e^{A_2 t_2^*}\left(e^{A_1 t_1^*}(x_1^* + A_1^{-1}B_1) - A_1^{-1}B_1 + A_2^{-1}B_2\right) - A_2^{-1}B_2$$

which, after solving for x_1^*, gives the desired result. Since $x_1^* \in S_1$, $g_1 = C_1 x_1^* + d_1 = 0$. x_2^* and g_2 can be found in a similar way. ∎

Proof of proposition 2.2: Integrating the linear dynamics between two switching surfaces yields

$$x_{i+1}^* = E_i x_i^* + (E_i - I)z_i$$

To find x_{k+1}^* as a function of x_1^*, solve recursively:

$$\begin{aligned} x_{k+1}^* &= E_k x_k^* + (E_k - I)z_k \\ &= E_k\left(E_{k-1}x_{k-1}^* + (E_{k-1} - I)z_{k-1}\right) + (E_k - I)z_k \\ &= E_k E_{k-1}x_{k-1}^* + E_k(E_{k-1} - I)z_{k-1} + (E_k - I)z_k \\ &= E_k \cdots E_1 x_1^* + E_k \cdots E_2(E_1 - I)z_1 + \cdots + E_k E_{k-1} \\ &\quad (E_{k-2} - I)z_{k-2} + E_k(E_{k-1} - I)z_{k-1} + (E_k - I)z_k \end{aligned}$$

The desired result can be obtained by noticing $x_{k+1}^* = x_1^*$ and solving for x_1^*. g_1 can be found by computing $g_1 = C_1 x_1^* + d_1 = 0$, since $x_1^* \in S_1$. The rest of the proof follows in a similar way. ∎

Proof of proposition 2.3: Theorem 3.1 in [1] proves this proposition for $k = 1$. Following a similar argument, consider a trajectory with initial condition $x(0) = x_1^*$. Then, the solution at time t_1^* is $x(t_1^*) = x_2^* = e^{A_1 t_1^*}(x_1^* + A_1^{-1}B_1) - A_1^{-1}B_1$. Now, let $x(0) = x_1^* + \delta_1 x_1^*$ where $\delta_1 x_0^*$ is chosen so that $x(0) \in S_1$. Thus, from the proof of theorem 3.1 in [1],

$$x(t_1^* + \delta_1 t_1^*) = x_2^* + W_1 \delta_1 x_1^* + O(\delta_1^2)$$

Similarly,

$$x(t_2^* + \delta_2 t_2^*) = x_3^* + W_2 \delta_2 x_2^* + O(\delta_2^2)$$

with initial condition $x_2^* + \delta_2 x_2^* = x_2^* + W_1 \delta_1 x_1^* + O(\delta_1^2)$. Neglecting high-order terms, we get $\delta_2 x_2^* = W_1 \delta_1 x_1^*$. Replacing in the above equality yields

$$x(t_2^* + \delta_2 t_2^*) = x_3^* + W_2 W_1 \delta_1 x_1^* + O(\delta_1^2)$$

Repeating this procedure $k-2$ times, we get to the last system, system k. Letting the initial condition to system k be $x_k^* + \delta_k x_k^* = x_k^* + W_{k-1} \cdots W_2 W_1 \delta_1 x_1^* + O(\delta_1^2)$ leads to

$$\begin{aligned} x(t_k^* + \delta_k t_k^*) &= x_{k+1}^* + W_k \delta_k x_k^* + O(\delta_k^2) \\ &= x_1^* + W_k W_{k-1} \cdots W_2 W_1 \delta_1 x_1^* + O(\delta_1^2) \end{aligned}$$

where we used the fact $x_{k+1}^* = x_1^*$. This proves the proposition. ∎

Proof of lemma 3.1: Since the limit cycle is transversal at switching surfaces, impact map i is continuous in some neighborhood of x_i^* in S_i. Any trajectory starting in this neighborhood intersects S_{i+1} transversally. The idea is to find which points in S_i result in tangent trajectories at S_{i+1}. Let $y(t) = C_{i+1}x(t) - d_{i+1}$ with $x(0) = x_i^* + \Pi_i \Delta_i \in S_i$. Thus, the points that result in tangent trajectories are those that $\dot{y}(t) = 0$. Note that $y(t) = C_{i+1}x(t) - d_{i+1} = C_{i+1}e^{A_i t}\Pi_i \Delta_i + C_{i+1}x_i^*(t) - d_{i+1} = C_t \Delta_i - d_t$. Hence, $\dot{y}(t) = 0$ are those points such that $\dot{C}_t \Delta_i = \dot{d}_t$. The final step is to find the largest ellipsoid $\|\Delta_i\|_{P_i}$ that does not intersect the hyperplane $\dot{C}_t \Delta_i = \dot{d}_t$. The radius of such ellipse is given by R_i^c. The proof, omitted here, is based on making the ellipse tangent to the hyperplane. ∎

Proof of lemma 3.2: From above, and using the fact $y(t) = 0$, it follows that $C_t \Delta_i = d_t$. Dividing and subtracting the right side of the equality by $t - t_i^*$, and taking the absolute value leads to

$$\left|\frac{d_t}{t - t_i^*}\right| |t - t_i^*| = \left|C_t \Delta_i\right| \leq \|C_t'\|_{P_i^{-1}} \|\Delta_i\|_{P_i}$$

or

$$|t - t_i^*| \leq \frac{\|C_t'\|_{P_i^{-1}}}{\left|\frac{d_t}{t - t_i^*}\right|} \|\Delta_i\|_{P_i} = \frac{1}{f(t)} \|\Delta_i\|_{P_i}$$

for all Δ_i and $t = \tilde{t}(\Delta_i)$. It is easy to see that if $\Delta_i = 0$ then $t - t_i^* = 0$. Now, due to the fact that $f(t)$ is continuous on $[t_i^* - r, t_i^* + r]$ (for small enough r), one can find an $\hat{R} > 0$ small enough such that

$$\|\Delta_i\|_{P_i} \leq \hat{R} \Rightarrow |t - t_i^*| \leq r \tag{9}$$

because a small increase in $\|\Delta_i\|_{P_i}$ must correspond to a small increase in $|t - t_i^*|$. Let $\hat{R} = \min_{t - t_i^* \in [-r, r]} f(t)\hat{r}$ where $0 < \hat{r} \leq r$ is small enough. Then $\|\Delta_i\|_{P_i} \leq \hat{R} \Rightarrow |t - t_i^*| \leq \hat{r}$.

Now, if we increase $\hat{r}$ to r, we have $|t - t_i^*| \leq r$ which means that (9) is not violated. Therefore we found $\bar{R}_i = \min_{t - t_i^* \in [-r, r]} f(t)r$ for which $\|\Delta_i\|_{P_i} < R_i \Rightarrow |t - t_i^*| \leq r$. ∎

Proof of lemma 3.3: Let $\bar{R}_i \geq 0$ be such that $\bar{R}_i^2 (C_t P_i^{-1} C_t') \leq d_t^2$ for all $t \notin [t_{i-}, t_{i+}]$. By contradiction, we want to show

that $\|\Delta_i\|_{P_i} \geq R_i$ if $t \notin [t_{i-}, t_{i+}]$. Following a similar argument from the previous proof, $y(t) = 0 \Rightarrow C_t\Delta_i = d_t$. For some $t \notin [t_{i-}, t_{i+}]$, a possible parametrization of Δ_i is

$$\Delta_i = \frac{P_i^{-1}C_t'}{C_tP_i^{-1}C_t'}d_t + C_t^{\perp}z_i$$

where $z_i \in \mathbb{R}^{n-2}$. Then

$$\begin{aligned}\Delta_i'P_i\Delta_i &= d_t\frac{C_tP_i^{-1}}{C_tP_i^{-1}C_t'}P_i\frac{P_i^{-1}C_t'}{C_tP_i^{-1}C_t'}d_t + 2\frac{C_tP_i^{-1}}{C_tP_i^{-1}C_t'}P_iC_t^{\perp}z_i \\ &\quad + (C_t^{\perp}z_i)'P_iC_t^{\perp}z_i \\ &= \frac{d_t^2}{C_tP_i^{-1}C_t'} + 2\frac{C_t}{C_tP_i^{-1}C_t'}C_t^{\perp}z_i + (C_t^{\perp}z_i)'P_i(C_t^{\perp}z_i) \\ &\geq R_i^2\end{aligned}$$

where in the first term we used the assumption that $d_t^2 \geq R_i^2(C_tP_i^{-1}C_t')$, the second term is zero since $C_tC_t^{\perp} = 0$ by definition, and in the last term $P_i > 0$. ■

A geometric interpretation of the above proof is as follows. Given $R_i \geq 0$, the set $\{x_i^* + \Pi_i\Delta_i : \|\Delta_i\|_{P_i} < R_i\}$ defines an ellipsoid in the switching surface S_i (see figure 5). Let $t \notin [t_{i-}, t_{i+}]$. The set $C_t\Delta_i = d_t$ defines an $n-2$ dimensional hyperplane in S_i. Draw the two hyperplanes parallel to the hyperplane $C_t\Delta_i = d_t$ and tangent to the ellipsoid, i.e., the hyperplanes $C_t\Delta_i = \pm d_x$, where $d_x = R_i\sqrt{C_tP_i^{-1}C_t'}$. To guarantee that the hyperplane $C_t\Delta_i = d_t$ does not intersect the ellipsoid it is necessary and sufficient that $d_t \geq d_x$.

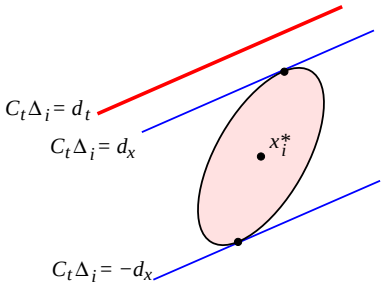

Fig. 5. Geometric interpretation of lemma 3.3

VI. CONCLUSIONS

This paper presented conditions that characterize regions of stability around locally stable limit cycles of piecewise linear systems (PLS). These help better understand numerous technological and biological applications that exhibit limit cycle oscillations. The results were divided in two steps. *Step 1* found the largest sets of switching times for each impact map. Then, *Step 2* searched for reasonable large regions at each switching surface, characterizing a contraction region around the limit cycle.

VII. REFERENCES

[1] Karl J. Åström. Oscillations in systems with relay feedback. *The IMA Volumes in Mathematics and its Applications: Adaptive Control, Filtering, and Signal Processing*, 74:1–25, 1995.

[2] Jorge M. Gonçalves, Alexandre Megretski, and Munther A. Dahleh. Global analysis of piecewise linear systems using impact maps and surface Lyapunov functions. *IEEE Transactions on Automatic Control*, November 2003.

[3] Didier Gonze, José Halloy, Jean-Christophe Leloup, and Albert Goldbeter. Stochastic models for circadian rhythms: effect of molecular noise on periodic and chaotic behavior. *C. R. Biologies*, 326:189–203, 2003.

[4] Arash Hassibi and Stephen Boyd. Quadratic stabilization and control of piecewise linear systems. In *ACC, Philadelphia, Pennsylvania*, June 1998.

[5] Jianjuen J. Hu. *Stable locomotion control of bipedal walking robots: synchronization with neural oscillators and switching control*. PhD thesis, Massachusetts Institute of Technology, Cambridge, MA, September 2000.

[6] J. Imura and A. van der Schaft. Characterization of well-posedness of piecewise-linear systems. *IEEE Transactions on Automatic Control*, 45(9):1600–1619, Sept 2000.

[7] Mikael Johansson and Anders Rantzer. Computation of piecewise quadratic Lyapunov functions for hybrid systems. *IEEE Transactions on Automatic Control*, 43(4):555–559, April 1998.

[8] James Keener and James Sneyd. *Mathematical Physiology*. Springer-Verlag, New York, 1998.

[9] Kiyotoshi Matsuoka. Sustained oscillations generated by mutually inhibiting neurons with adaptation. *Biological Cybernetics*, 52:367–376, 1985.

[10] Pablo A. Parrilo. *Structured Semidefinite Programs and Semialgebraic Geometry Methods in Robustness and Optimization*. PhD thesis, California Institute of Technology, Pasadena, CA, 2000.

[11] Stefan Pettersson and Bengt Lennartson. An LMI approach for stability analysis of nonlinear systems. In *ECC, Brussels, Belgium*, July 1997.

[12] Robert P. Ringrose. *Self–stabilizing running*. PhD thesis, Massachusetts Institute of Technology, Cambridge, MA, February 1997.

[13] M. Rubensson and B. Lennartson. Stability of limit cycles in hybrid systems using discrete-time lyapunov techniques. In *CDC*, Sydney, Australia, 2000.

[14] Matthew M. Williamson. *Robot Arm Control Exploiting Natural Dynamics*. PhD thesis, Massachusetts Institute of Technology, Cambridge, MA, June 1999.